

2004

# Influence of Antenna Aiming on ECE in MAST

Josef Preinhaelter

Jakub Urban

Pavol Pavlo

Vladimir Shevchenko

Martin Valovič

*See next page for additional authors*

Follow this and additional works at: [https://digitalcommons.odu.edu/ece\\_fac\\_pubs](https://digitalcommons.odu.edu/ece_fac_pubs)

 Part of the [Electrical and Computer Engineering Commons](#), and the [Plasma and Beam Physics Commons](#)

## Repository Citation

Preinhaelter, Josef; Urban, Jakub; Pavlo, Pavol; Shevchenko, Vladimir; Valovič, Martin; Vahala, Linda L.; and Vahala, George, "Influence of Antenna Aiming on ECE in MAST" (2004). *Electrical & Computer Engineering Faculty Publications*. 30.  
[https://digitalcommons.odu.edu/ece\\_fac\\_pubs/30](https://digitalcommons.odu.edu/ece_fac_pubs/30)

## Original Publication Citation

Preinhaelter, J., Urban, J., Pavlo, P., Shevchenko, V., Valovic, M., Vahala, L., & Vahala, G. (2004). Influence of antenna aiming on ECE in MAST. *Review of Scientific Instruments*, 75(10), 3804-3806. doi: 10.1063/1.1783601

---

**Authors**

Josef Preinhaelter, Jakub Urban, Pavol Pavlo, Vladimir Shevchenko, Martin Valovič, Linda L. Vahala, and George Vahala

## Influence of antenna aiming on ECE in MAST

Josef Preinhaelter, Jakub Urban, and Pavol Pavlo  
*EURATOM/IPP.CR Association, Institute of Plasma Physics, Prague, Czech Republic*

Vladimir Shevchenko and Martin Valovič  
*EURATOM/UKAEA Fusin Association, Culham Science Centre, Abingdon, United Kingdom*

Linda Vahala  
*Old Dominion University, Norfolk, Virginia 23529*

George Vahala  
*College of William and Mary, Williamsburg, Virginia 23185*

(Presented on 20 April 2004; published 7 October 2004)

The effect of the direction of the detected beam on the intensity of ECE is studied. It is found that the combined effects of the strong dependence of the conversion efficiency of O mode at the plasma resonance on the direction of the incident wave and the partial screening of the beam waist by the MAST vessel wall, can be responsible for the weakening of ECE emission for some frequencies. The theoretical model for ECE data interpretation on MAST has been significantly improved. New features of the model are as follows: the quasioptical treatment of the receiving antenna, interference, polarization and screening effects of the vacuum window and collisional damping of EBWs in the peripheral plasma. © 2004 American Institute of Physics.  
 [DOI: 10.1063/1.1783601]

### I. INTRODUCTION

Extensive ECE data from 16 to 60 GHz are available in MAST.<sup>1</sup> The characteristic low magnetic field and high plasma density of a spherical tokamak do not permit the typical radiation of O and X modes from the first five electron cyclotron harmonics. Thus only electron Bernstein modes, (modes not subject to a density limit), which mode convert into electromagnetic waves in the upper hybrid resonance region, can be responsible for the measured radiation.<sup>2</sup>

The instantaneous magnetic field and its spatial derivatives are reconstructed from 2D splining of two potentials determined by an EFIT equilibrium reconstruction code, assuming toroidal symmetry. The plasma density and temperature profiles in the whole RZ cross section of the plasma are obtained from mapping the high spatial resolution Thomson scattering measurements onto magnetic surfaces. We improved our 3D plasma model in Ref. 3 by the inclusion of complete MAST ECE antenna geometry (see Fig. 1). We use the Gaussian beam formalism to find the waist positions (one in horn and the second in front of the window) between mirrors (see Fig. 2). Only linearly polarized waves are detected by our radiometer and the plane of polarization can be selected by the orientation of the polarization rotator. At the mirrors the polarization follows the simple rule:

$$\mathbf{E}_{\text{ref}} = -\mathbf{E}_{\text{inc}} + 2N_m(\mathbf{E}_{\text{inc}} \cdot N_m),$$

where  $\mathbf{E}_{\text{inc}}$  and  $\mathbf{E}_{\text{ref}}$  are the incident and reflected fields and  $N_m$  is the normal to the mirror. At the window the waves are partly reflected and the linear polarization becomes slightly elliptical.

To simplify the computation we use a separate set of straight rays to project the rim of window and the visible

area onto the second waist plane. Such an approach takes into account the shape of the Gaussian beam in the near and far antenna regions. At the intersection of the rays with the last closed flux surface (spots) we consider an auxiliary plane stratified plasma slab which is inhomogeneous along the local density gradient. In this slab we solve Maxwell equations for wave propagation in a cold plasma by the finite element method with adaptive steps between nodes<sup>4</sup> (see Fig. 3). The power absorbed in the vicinity of the upper hybrid resonance due to weak collisions corresponds (if  $\nu/\omega \rightarrow 0$ ) exactly to the power converted to the electron Bernstein waves. The reverse process is appropriate for ECE because we can assume reciprocity between emission and absorption.

Two processes here play a role: the direct EBW-X conversion as well as the process in which an obliquely incident

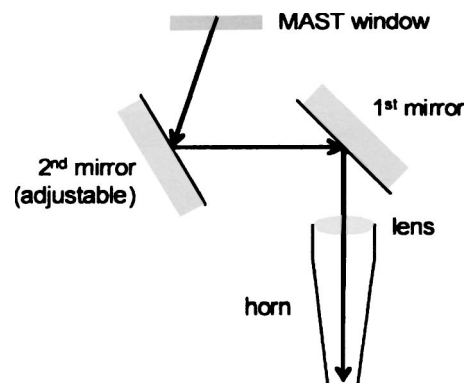


FIG. 1. ECE antenna on MAST. Ray between the second mirror and the window is inclined at  $\varphi_{\text{dev}}$  from the equatorial plane upward and the angle between its projection onto the equatorial plane and the vertical plane going through the tokamak axis and the antenna position is  $\varphi_{\text{long}}$ .

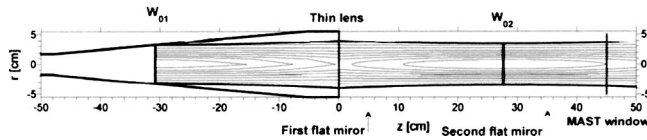


FIG. 2. Intensity of Gaussian beam in MAST antenna system for  $f = 40$  GHz;  $W_{01}$  and  $W_{02}$  are waist positions.

EBW is first converted to an X mode which subsequently mode converts to an O mode<sup>5</sup> at the plasma resonance. We also use this slab model to determine the position of the UHR nearest to each spot and to obtain here the solution of the electrostatic dispersion relation of the electron Bernstein waves (EBW). This solution serves as an initial condition for the standard ray tracing<sup>6</sup> describing the propagation of EBW in 3D.

To determine the radiative temperature for Rayleigh–Jeans black body radiation we must solve, for each ray, the radiative transfer equation simultaneously with the ray evolution equation. This approach takes into account the reabsorption of radiation which is important for nonlocal wave damping.

## II. SIMULATED ECE POWER DETECTED BY ANTENNA

The intensity of ECE detected by the antenna can be expressed as

$$I_{ECE} = \text{const} \times \iint dS W_{\text{Gauss}} C_{\text{EBW-X-O}} \omega^2 T_{\text{rad}} C_{\text{window}} V_{\text{relat}}$$

where the Gaussian weight  $W_{\text{Gauss}} = e^{-(2r^2/w_0^2)}$ ,  $w_0$  is the beam waist radius,  $C_{\text{EBW-X-O}}$  is the mode conversion efficiency,  $\omega^2 T_{\text{rad}}$  is the Rayleigh–Jeans back body radiation,  $C_{\text{window}}$  is the power transmission coefficient through the MAST window, and the relative visible area  $V_{\text{relat}} = w^2/w_0^2$  ( $w$  is the Gaussian beam radius at the plasma surface). The integration is taken over the intersection of the waist and the projection of the vessel window rim onto the waist plane.

In Fig. 4 we compare the experimentally detected ECE for discharge No. 7798 at  $t = 240$  ms, when the high spatial

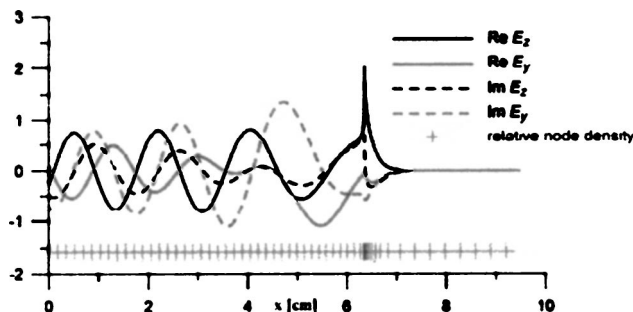


FIG. 3. Components of the wave electric field (arb. Units) in an inhomogeneous slab. There is a high density of nodes at the upper hybrid resonance,  $x \sim 0.065$  m.

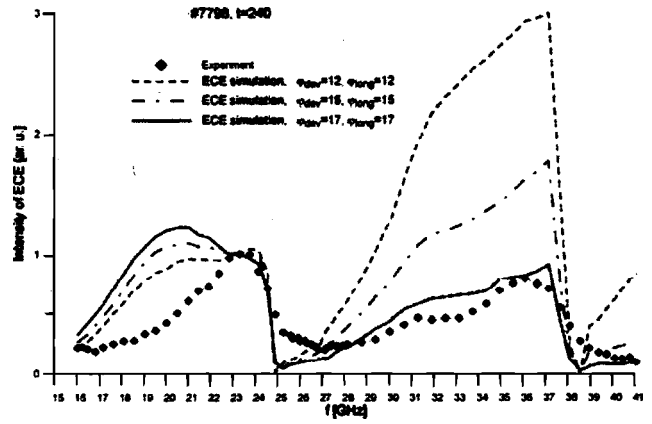


FIG. 4. ECE from MAST, shot No. 7798,  $t = 240$  ms. Reference frequency  $f = 23.14$  GHz, for which  $I_{ECE} = 1$ .

resolution Thomson scattering measurements of density and temperature are taken, with the simulations for three different orientations of the detected beams.

First we consider the detected beam with  $\varphi_{\text{dev}} = \varphi_{\text{long}} = 12^\circ$ . The discrepancy between the measured and the simulated results is striking (at 36.46 GHz the simulated value is 3 times higher than the experimental value). We now investigate some possible reasons for this discrepancy. For shot No. 7798, the conversion region for low frequency waves is situated in the highly turbulent plasma scrapoff layer. Under these conditions mode conversion is weak and nonrobust. So we exclude these waves with frequencies in the range 15–22 GHz from further consideration.

At the plasma boundary where the temperature is low and the density sufficiently high collisions could play an important role. On incorporating collisions into the EBW dispersion under the BGK approximation,<sup>7</sup> we found only weak effects, even at  $Z_{\text{eff}} = 4$ .

We also investigated the effect of the polarization of the detected wave. From the results shown in Fig. 5, we see that the peak at 36.46 GHz is three times higher irrespective of the wave polarization.

The last important quantity, which could influence the intensity of detected emission, is beam directionality. The

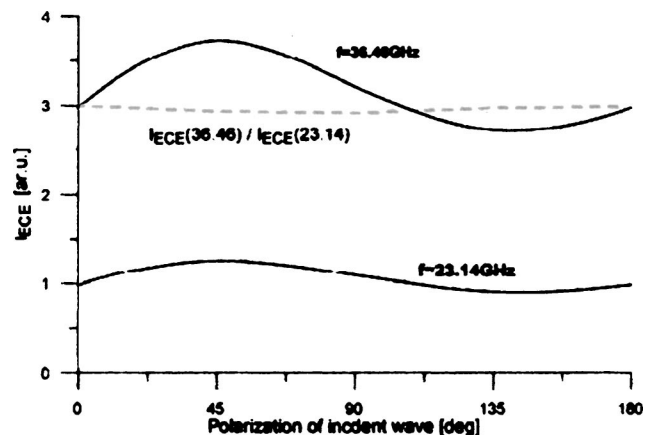


FIG. 5.  $I_{ECE}$  as a function of the angle between the electric field of the linearly polarized wave in the horn mouth and the equatorial plane: No. 7798,  $\varphi_{\text{dev}} = \varphi_{\text{long}} = 12^\circ$ .

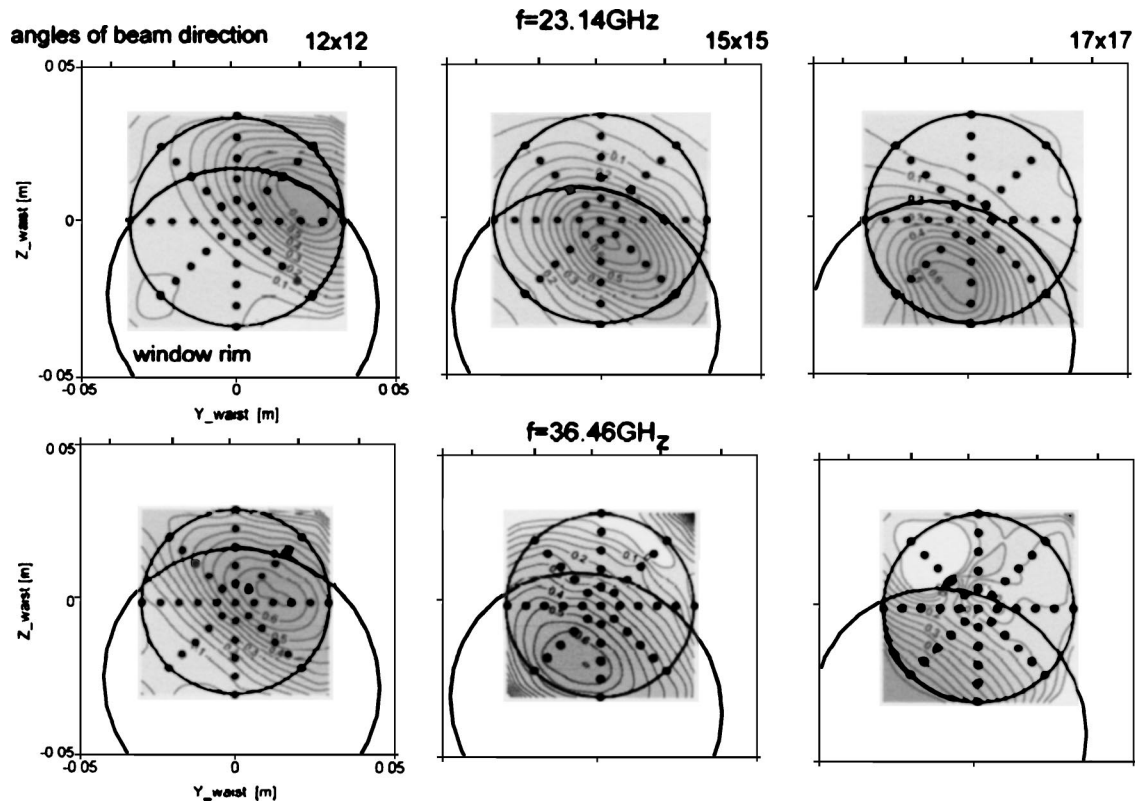


FIG. 6. Contour maps of the conversion efficiency projected onto the Gaussian beam waist plane for No. 7798,  $t=240$  ms as derived from our code. The dots correspond to the individual rays, the circle forms the boundary of the beam waist and the ellipse segment is a rim of the MAST window projected onto the plane of the waist.

power of the O-mode transmitted through the plasma resonance region depends strongly on the direction of the incident wave:

$$T = \exp \left( - \frac{\pi k_{\text{vac}}}{4 \kappa_p} \left( \frac{2\omega}{\omega_{ce}} \right)^{1/2} \left\{ \frac{\omega_{ce}^2}{\omega^2} \left[ 1 - \left( \frac{N_z^{\text{inc}}}{N_z^{\text{opt}}} \right)^2 \right]^2 + \frac{2\omega_{ce}}{\omega} (N_y^{\text{inc}})^2 \right\} \right),$$

where  $N_z^{\text{opt}} = [\omega_{ce}/(\omega + \omega_{ce})]^{1/2}$  and  $z$  denotes the direction of the total magnetic field at the plasma resonance.<sup>8</sup> We thus

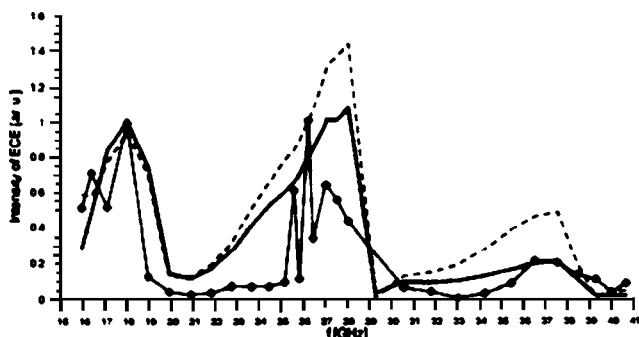


FIG. 7. ECE from MAST, shot No. 4958,  $t=120$  ms. Reference frequency  $f=17.94$  GHz, for which  $I_{\text{ECE}}=1$ . The diamonds are experimental points, the full line (best fit) corresponds to  $\varphi_{\text{dev}}=18^\circ$ ,  $\varphi_{\text{long}}=22^\circ$  and the dashed line to the original  $\varphi_{\text{dev}}=16^\circ$ ,  $\varphi_{\text{long}}=20^\circ$ .

suspect that the conversion efficiency will be sensitive to small changes in the directions of the detected beams.

To verify this, we plot the conversion efficiency projected onto the waist plane for both peaks (23.14 and 36.46GHz) and three choices of  $(\varphi_{\text{dev}}, \varphi_{\text{long}})$ : the original ( $12^\circ$  and  $12^\circ$ ), and then ( $15^\circ$  and  $15^\circ$ ), and the choice ( $17^\circ$  and  $17^\circ$ ) that gives the best fit to experiment, see Fig. 6. We see, that for the wave with  $f=36.46$  GHz, the conversion efficiency maximum (0.6) is situated at the center of the waist at  $\varphi_{\text{dev}}=12^\circ$ ,  $\varphi_{\text{long}}=12^\circ$  but for  $\varphi_{\text{dev}}=17^\circ$ ,  $\varphi_{\text{long}}=17^\circ$  the rim of the window crosses the waist center and the conversion efficiency is small (0.1–0.2). This decrease in the conversion efficiency to the  $I_{\text{ECE}}$  results in a better agreement between the simulated and measured data as plotted in Fig. 4 for  $\varphi_{\text{dev}}=17^\circ$ ,  $\varphi_{\text{long}}=17^\circ$ . It is thus possible that the actual directionality of the detected beam is ( $17^\circ$  and  $17^\circ$ ) rather than the originally supposed ( $12^\circ$  and  $12^\circ$ ). A similar situation also arises for the shot No. 4958, although in this shot the beam directionality error can be estimated at  $2^\circ$  (see Fig. 7).

<sup>1</sup> V. Shevchenko, 15th rf Power in Plasma, Moran (2003), p. 359.

<sup>2</sup> H. P. Laqua, 15th rf Power in Plasma, Moran (2003), p. 15.

<sup>3</sup> J. Preinhaelter, 15th rf Power in Plasma, Moran (2003), p. 388.

<sup>4</sup> J. Urban and J. Preinhaelter, Czech. J. Phys. **54**, Suppl. C, C109 (2004).

<sup>5</sup> J. Preinhaelter and V. Kopecky, J. Plasma Phys. **10**, 1 (1973).

<sup>6</sup> P. Pavol and L. Krlin, Nucl. Fusion **31**, 711 (1991).

<sup>7</sup> S. Petic, Physica C **125**, 118 (1985).

<sup>8</sup> J. Preinhaelter, Czech. J. Phys. **45**, 399 (1995).